NRIAG Journal of Astronomy and Geophysics 6 (2017) 90–96

Contents lists available at ScienceDirect

NRIAG Journal of Astronomy and Geophysics

journal homepage: www.elsevier.com/locate/nrjag

Full length article

Study of Conrad and Shaban deep brines, Red Sea, using bathymetric, parasound and seismic surveys

Mohamed Salem

Geology Department, Faculty of Science, Benha University, Egypt

ARTICLE INFO

Article history:
Received 24 March 2017
Revised 1 April 2017
Accepted 10 April 2017
Available online 26 April 2017

ABSTRACT

Red Sea was formed where African and Arabian plates are moving apart. Each year the plates drift about 2.5 cm farther apart, so that the Red Sea is slowly but steadily growing hence known as the next coming ocean simply an embryonic ocean. It is characterized by the presence of many deep fractures, located almost exactly along the middle of the Sea from northwest to southeast. Theses fractures have steep sides, rough bottom and brines coming up form on the bottom. Brine deposits are the result of subsurface magmatic activity. They are formed in graben structure as shown by the bathymetric, parasound and seismic studies in the investigated area.

© 2017 Production and hosting by Elsevier B.V. on behalf of National Research Institute of Astronomy and Geophysics. This is an open access article under the CC BY-NC-ND license (http://creativecommons.org/licenses/by-nc-nd/4.0/).

1. Introduction

Narrow marginal shelves and coastal plains are the main morphological features of the Red Sea. The main trough of the Red Sea is broad with depth about 400–1100 m. The main trough of the southern Red Sea is bisected by ~60 km wide axial trough, about 2000 m deep. The early Red Sea was formed about 30 Ma ago where African and Arabian plates were close forming one plate before moving apart (Roeser, 1975; Girdler and Southern, 1987). The axial trough of the Red Sea between15°N to 19°30′N was occupied by the well-developed magnetic anomalies of the seafloor spreading center (Roeser, 1975 and Cochran, 1983). North and south of the Red Sea spreading was prevailed from this center (Roeser, 1975 and Cochran, 1983). At the north of 19°30′N; the bottom of the Red Sea is divided into rough topography reflecting high and low zones. These zones reflect NE-SW short faults nearly 5 km in length (Cochran, 1983). The Red Sea deeps are isolated by broader and shallower inter-trough zones. These zones covered by Miocene evaporites and post-Miocene sediments (Izzeldin, 1989).

The northern 500 km of the Red Sea has bathymetrically surveyed stepping down to an axis of deep water. Sediments in this region are faulted and deformed (Cochran and Martinez, 1988). Small deeps are generally associated with large dipolar magnetic anomalies which they spaced along the axial depression (Pautot et al., 1986; Cochran et al., 1986). The deeps of the central Red Sea transition zone are much larger than the deeps accompanied with dipolar magnetic anomalies. The small deeps, e.g. Shaban Deep, have sediments in the bottom which are intruded by igneous rocks (Pautot et al., 1984).

The purpose of this paper is to present new detailed bathymetric maps to the elongated deeps which are called Conrad and Shaban Deeps (Fig. 1). These deeps are studied with seismic and parasound surveys. The present data are worked out by a Cruise Meteor M44/3 in 1999 and processed in the laboratories of Bremen University, Germany. The results of this work were amended by previous published works in the conclusion of present study.

2. Methodology

The data used in the Conrad Deep studies have been acquired in 1999 during the Meteor Cruise 44/3. The survey by Hydrosweep and Parasound sediments echosounders are continuously operated to study the morphology, depositional processes and sediment structures of the seafloor. Multichannel seismic reflection survey is also used. The acquired data are digitally recorded in the present study.

The general objective of the multibeam Hydrosweep echosounder system is to survey the seafloor topographic features. A sector beam of 90° is covered by a fan of 59 pre-formed beams.

E-mail address: mohamedsalem199373@gmail.com

Peer review under responsibility of National Research Institute of Astronomy and Geophysics.

Production and hosting by Elsevier

http://dx.doi.org/10.1016/j.nrjag.2017.04.003

2090-9977/© 2017 Production and hosting by Elsevier B.V. on behalf of National Research Institute of Astronomy and Geophysics.
This is an open access article under the CC BY-NC-ND license (http://creativecommons.org/licenses/by-nc-nd/4.0/).

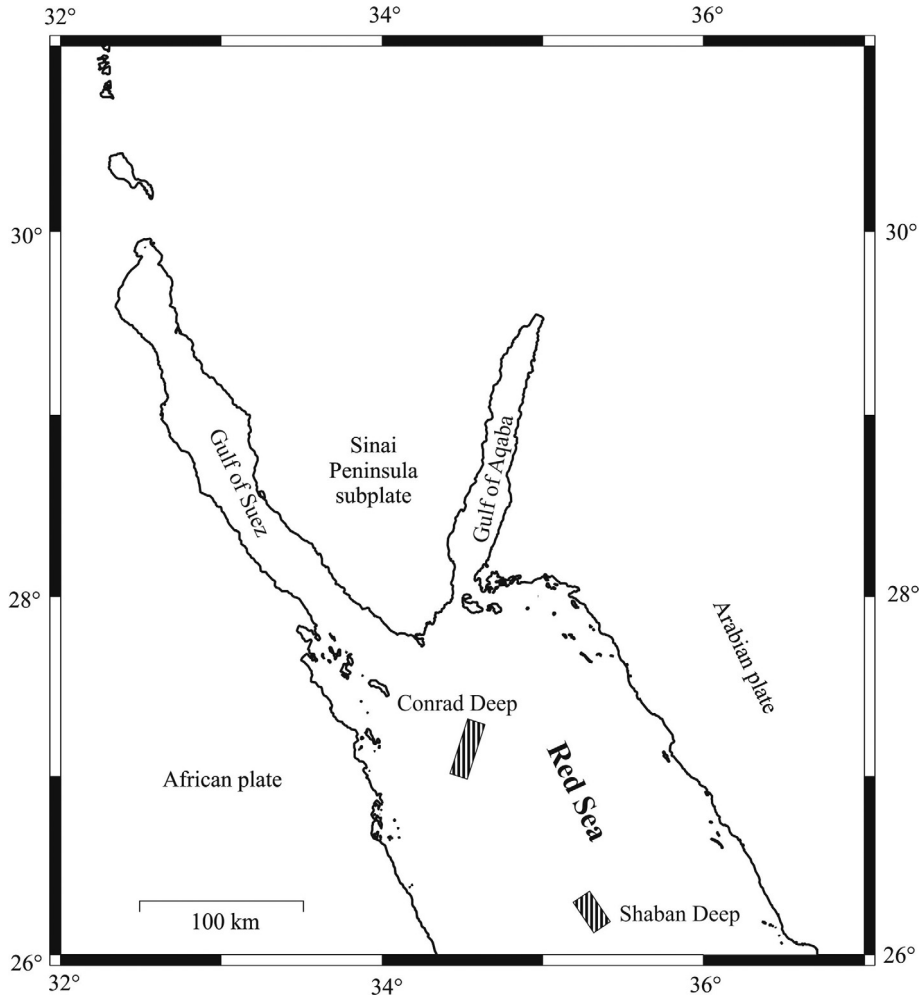

Fig. 1. Overview map of the study area (Conrad and Shaban Deeps). Location of detailed investigated area is shown by the above two boxes.

Consequently, a bar with the width of two times the water depth, perpendicular to the ship track, is mapped. Multibeam-system (mb-system) software package was used to process the data. This package consists of more than 20 programs. This mb-system software manipulate, translate, process, list, and display swath-mapped sonar data (Caress and Chayes, 1996). The data were finally were gridded with 70 m grid-size and displayed by the software of the Generic Mapping Tools (Wessel and Smith, 1999).

The uppermost seafloor sedimentary layers were surveyed with echo-sounder Parasound system. A very high vertical resolution is attained due to the narrow beam angle of 4°, the high signal frequency of 4 kHz, the short signal length of two sinoid pulses. The resolution of small horizontal changes is detected by an optimized succession generation of signals. The Parasond system data are analog which were converted to digital data. These data were stored on 9-track tapes or hard disks in a format of SEG-Y such as format with ParaDigma system (Spieß, 1993).

Multichannel seismic reflection measurements were accomplished with the instrumentation of the Marine and Environments Research Institute, Bremen University. Two seismic sources of different volumes were used, in an exchanging mode for some profiles. The first seismic source is the water gun (SODERA Inc. S-15) with a frequency range 200–2000 Hz gives information of the upper 100–300 m of the sediment succession. The second seismic source is the air gun (Generator-Injector Gun; SODERA Inc.). It has signal energy up to 350 Hz admits seismic imaging of sedimentary layers 1500 m, down seafloor depth.

3. Results and discussion

The Conrad deep area (Fig. 2) is bounded by latitude 34°38′ E–34°48′E and longitude 26°54′N–27°09′N and comprise an area about 30 km × 15 km. Conrad basin has an oval shape with longitudinal axis oriented approximately NE-SW, i.e. the same trend of the Gulf of Aqaba. The deepest part in Conrad area is 1550 m occupying about 10 km^2 in a total of 450 km^2. The depth decreases in the out direction to reach about 1000 m.

The Shaban area (Fig. 3) is approximately 25 km × 15 km (latitude 35°14′E–35°22′E and longitude 26°06′N–26°19′N) and comprises the second basin (Shaban basin). It was surveyed also using a multibeam “Hydrosweep”.

Shaban basin has extension (NW-SE, i.e. the same direction of the Gulf of Suez. The deepest part in Shaban area is 1600 m occupying about 40 km^2 in a total 375 km^2. The depth decreases in the out direction to reach about 950 m.

The bathymetric and the Parasound profiles show that the axial depression of the northern Red Sea becomes visible as a fault bounded graben. Extension of the northern Red Sea has reached a point at which the magma starts to erupt. The magma ascends along the faults bounding the axial depression.

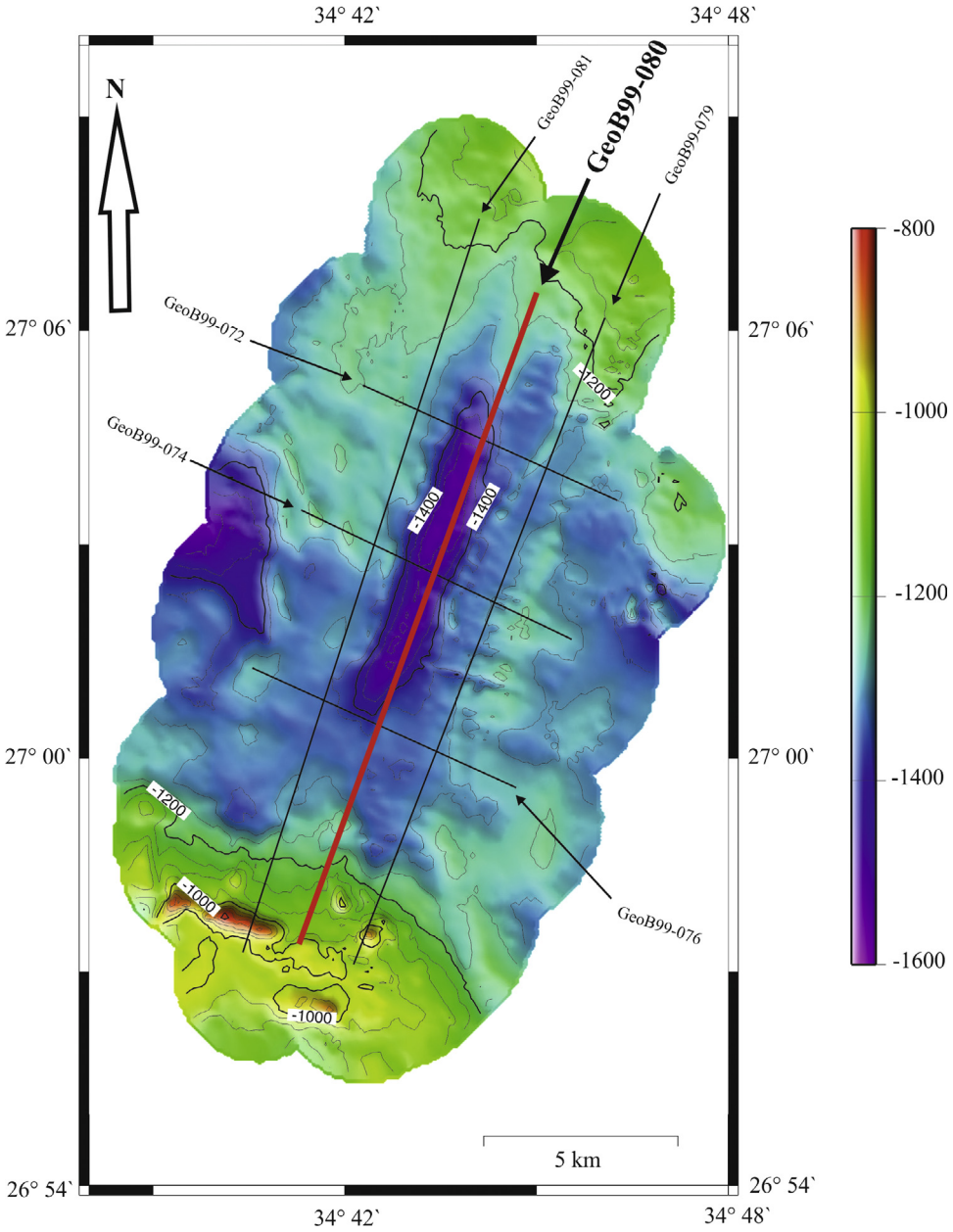

Fig. 2. Bathymetric map of the Conrad Deep. The Seismic and Parasound profiles are shown by straight lines. The selected profile (GeoB99-80) is shown by bold straight line.

The Parasound data from Conrad (Fig. 4) and Shaban (Fig. 5) Deeps shows diffusions of the reflections from the bottom of the depression. The top of brine sediments causes a sharp signal (GeoB99-080 & GeoB99-086) penetrating ~70 m deep. The shoulders of the depression show hummocky reflection pattern.

The Parasound reflection in the northern Red Sea show gravels, wavy sand and minor clay sediments above the basal Miocene sediments. However, Searle and Ross (1975) and Izzeldin (1989) studied the southern part of the Red Sea and stated that the sediments here are relatively similar to the northern part of the Red Sea, richer in detrital material due to the dilution of the diagonstic carbonate materials. The dilution are took place by the terrigenous material brought in by the numerous wadis. The "deeps" in the south are isolated by "inter-trough zones" which are wider and shallower in depth than in northern part of the Red Sea. The inter-trough zones are covered with faulted sediments. These sediments are the Miocene evaporites and post-Miocene pelagic sediments.

The Plio-Quaternary sediment layers are disturbed by various deformations, whereas the intense deformations are well found around the ridge as the result of diapers. These deformations are also interpreted a result of ruptures of evaporite layers due to extension stresses.

Seismic profiles of Conrad (Fig. 6) and Shaban (Fig. 7) Deeps are generally characterized by depths in the ranges of 1100–1250 m and they have depressions which are bounded by scarps of height up to a few hundred meters. Bedding patterns of the reflectors clearly suggest several unconformities in the deposition which are probably due to tectonic activity, during the Miocene and Quaternary. The sediment thickness is approximately up to 750 m or at least 0.75 s reflection times. The sediments are completely covered the depressions. The brines are found in the Conrad and Shaban Deeps as show strong seismic amplitudes (Figs. 6 and 7).

As observed in Parasound and seismic profiles of Conrad and Shaban deeps, the diapirs, pierced their way upward, are connected with faulting and rifting.

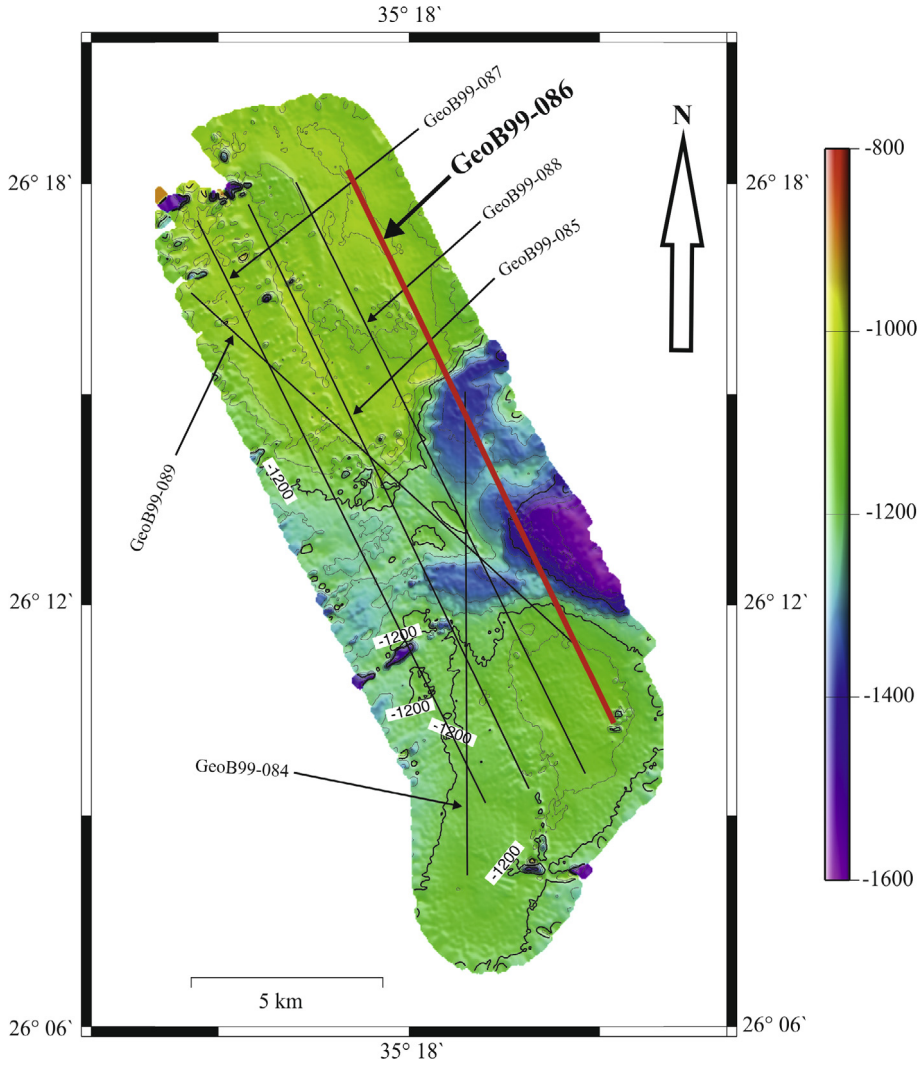

Fig. 3. Bathymetric map of the Shaban Deep. The Seismic and Parasound profiles are shown by straight lines. The selected profile (GeoB99-86) is shown by bold straight line.

Sketch (Fig. 8) shows brine-filled deeps which are located in the northern Red Sea (e.g. Shaban Deep brine) is plotted.

The hydrothermal brines evolution in Conrad and Shaban deeps are compared with other Red Sea deeps which were studied before by Makris and Rihm (1991), Carter and Hansen (1983), Shanks et al. (1977), Krauskopf (1957), David and Cronan (1980) and Winckler et al. (2000).

The Red Sea is one of the enclosed seas, so it is considered a unique environment. It has scarce rainfall and high evaporation. The values of salinity increase toward the North but decrease in value toward the South are due to the water exchange with the Indian Ocean, the mansoon rain during the summer time and the changing of freshwater from the east African rivers. The brine filled deeps are found along the central axis. The recorded high salinity values are due to leaching of subbottom salts of Miocene age (Makris and Rihm, 1991). Shaban and Conrad Deeps have also up to 200 m salt layers. This salt begins to dissolve and participates in the composition of the brines bodies themselves.

Carter and Hansen (1983) stated that the origin of diapirs is depending on temperature and pressure calculation at a depth of 1 km. They suggested that a confining lithostatic temperature is about 130 °C and pressure 30 MPa. Diapirism can be triggered by these high temperature and pressure values.

In general, the brines in the Red Sea bottom include several metalliferous sediments which include sulfides, oxides, carbonates, and silicates (Carter and Hansen, 1983). These types of metalliferous sediments are the product of a hydrothermal system arising from the circulation of seawater through evaporates and hot basalts along the Red Sea spreading center.

According to Shanks et al. (1977), the several metalliferous sediments are formed due to fractionation as the result of decreasing temperature of the brine after it emanates from the sea bottom and raising the activity of hydrogen ions (pH) and electrons (Eh). The sequence of precipitation of the metalliferous sediments, due to cooling, started with sulfides, iron silicates, iron oxides, and manganese oxides. Manganese deposits are precipitated later than iron oxides because of its rate of solubility and its oxidation at a higher pH (Krauskopf, 1957; David and Cronan, 1980).

Winckler et al. (2000) explained the brine evolution (Fig. 9). Red Sea deep water (RSDW) transferring the atmospheric noble gases penetrating the sediments. It becomes highly enriched in salt, during circulation through the Miocene evaporites. The temperature highly increases at the hydrothermal active zone, over the magma chamber. At this region, the brine is formed by reactions between Red Sea deep water, which enriched in salt and the hot young basalt in mid-ocean ridge basalts (MORBs) which enriched in He

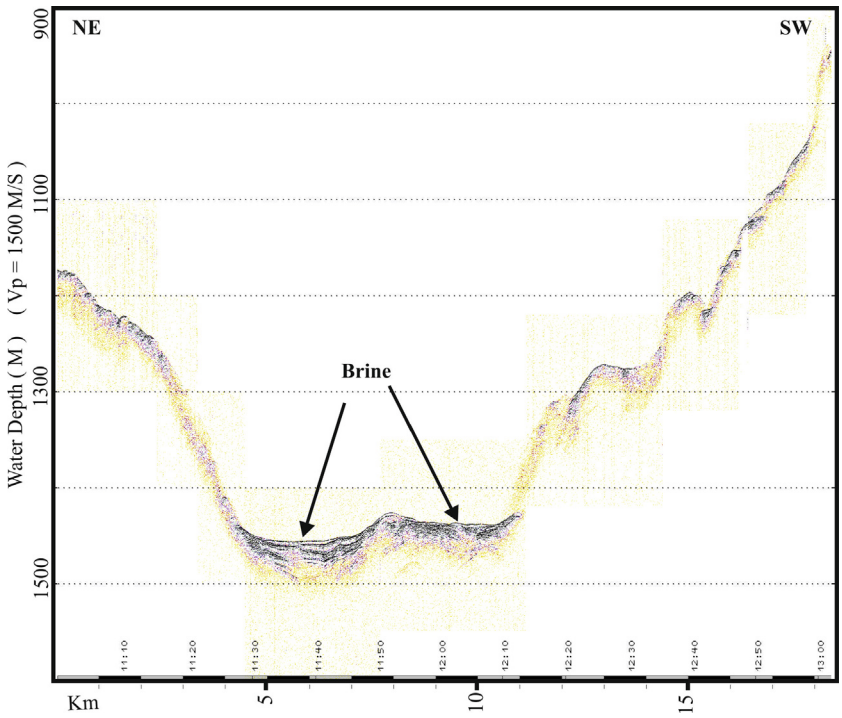

Fig. 4. Parasound profile GeoB99-080 cross Conrad Deep.

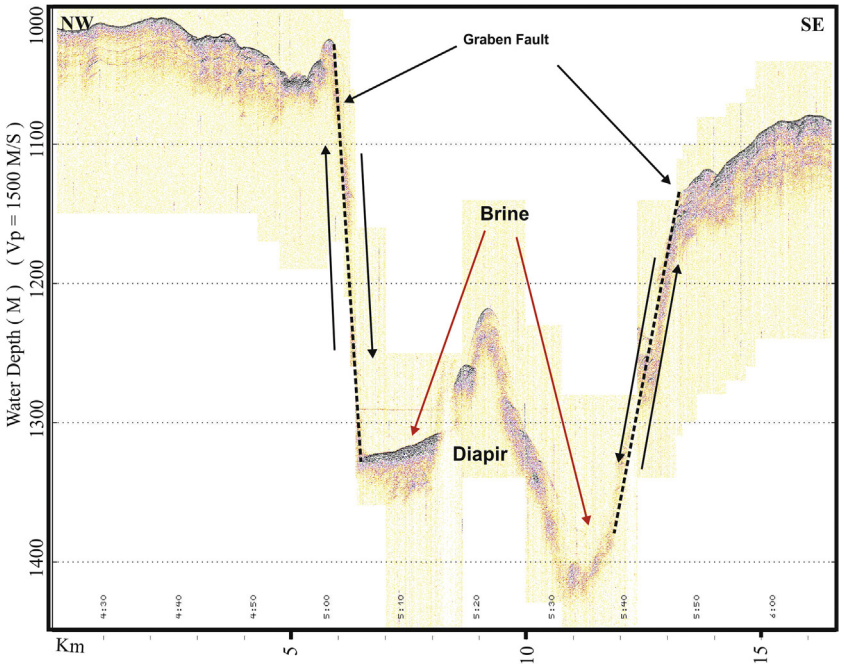

Fig. 5. Parasound profile GeoB99-086 cross Shaban Deep.

and Ar components. Boiled fluid is progressively ascending and moving into the direction of lower pressure regions. This fluid is divided into two phases, (1) a residual noble gas-depleted liquid phase and (2) a noble gas-enriched vapor phase. The residual fluid still has enriched He excess and noble gases. MORB–He excess as well as the atmospheric noble gases are depleted by boiling. The different noble gases are approximately gradually depleted at high temperatures. The gradual depletion is related to the differences in the solubility.

The residual depleted gases liquid is rapidly ascending to the sea floor and influx into the brine pool. The essential mixing of the sub surface with cold percolating sea water can be largely eliminated with respect to the top hot vent. So, the lower layer (LCL) seems essentially to represent the boiled fluid, whereby the upper

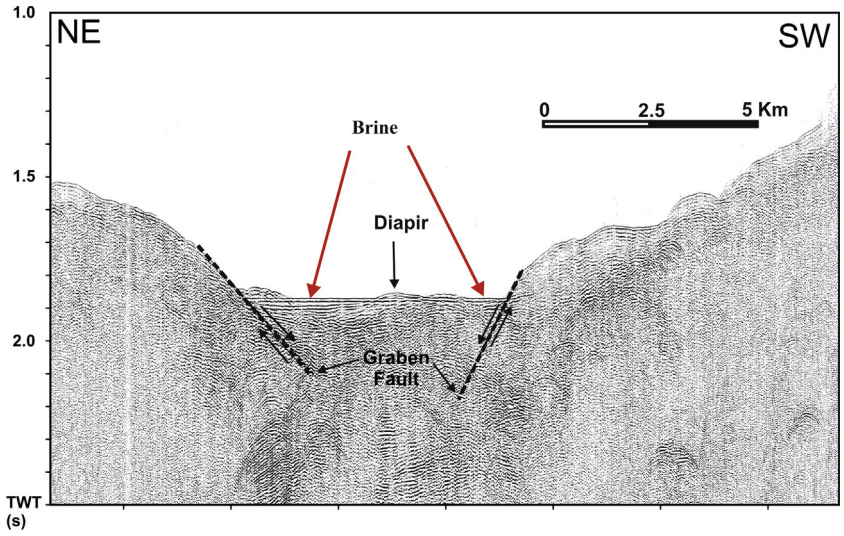

Fig. 6. Sesmic reflection profile GeoB99-080 cross Conrad Deep. It is showing a graben fault structure, brine and diapir that penetrated a rift floor.

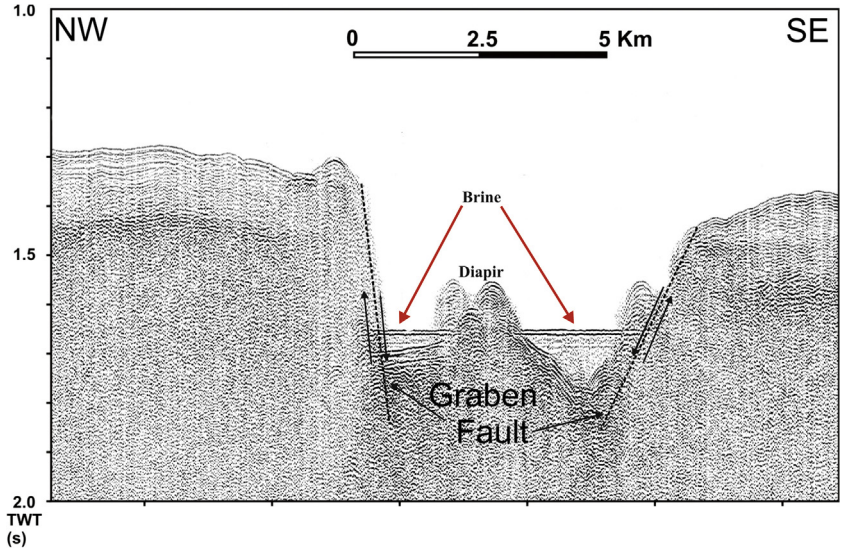

Fig. 7. Sesmic profile GeoB99-086 cross Shaban Deep. It is showing a graben fault structure, brine, salt diaper, penetrated the rift floor, underneath the block between the graben. The diaper is surrounded by the brine.

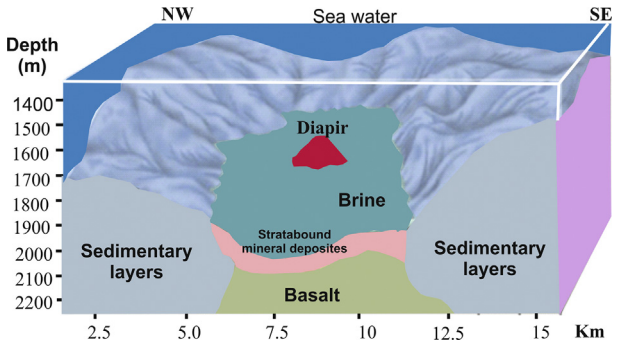

Fig. 8. Sketch showing Shaban Deep brine an example of northern Red Sea brines.

brine layers (UCL1, UCL2, UCL3. . .etc.) are formed as the result of subsequent mixing with RSDW.

4. Conclusion

This study with bathymetry, parasound and seismic surveys of Conrad and Shaban Deeps reveals that the brines are located in the Red Sea bottom, approximately 90 km southeast of the Gulf of Suez entrance. Both Conrad and Shaban Deeps are bounded by a well-defined wide axial graben faults. So, this study revealed that the deep brines are generated by the reaction between Red Sea deep water which enriched in salt, due to high evaporation and closed sea, and fluids produced by the magmatic injections.

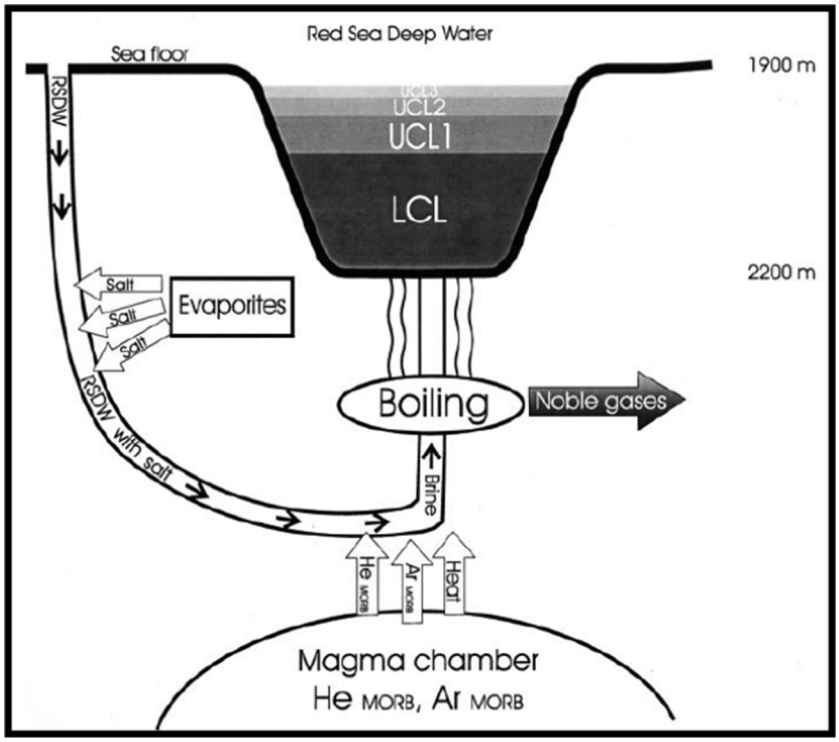

Fig. 9. Fantastic evolution model of the brine prior to injection into the Atlantis II Deep (after Winckler et al., 2000).

The Conrad deep area has an oval shape with longitudinal axis oriented approximately NE-SW, i.e. the same trend of the Gulf of Aqaba. The deepest point in the basin is about 1550 m. The Shaban Deep is rhombic in shape and has extension NW-SE, i.e. the same direction trend of the Gulf of Suez. The deepest point is about 1600 m.

According to the echo-reflector characteristics and geometry, the sediments at the deeps are more deformed, varying in size from gravel to sand with fine sediments and carbonate sediments.

Acknowledgement

I would like to thank crews of M44/3, and our colleagues for their help during the cruise. I am also very grateful to Prof. Dr. Volkhard Spiess and Dr. Sebastian Krastel for their help during data processing.

References

Caress, D.W., Chayes, D.N., 1996. Improved processing of Hydrosweep DS multibeam data on the R/V Maurice Ewing. December 1996 18(6), 631–650.
Carter, N.L., Hansen, F.D., 1983. Creep of rocksalt. Tectonophysics 92, 275–333.
Cochran, J.R., Martinez, F., 1988. Evidence from the northern Red Sea on the transition from continental to oceanic rifting. Tectonophysics 153, 25–53.
Cochran, J.R., Martinez, F., Steckler, M.S., Hobart, M.A., 1986. Conrad deep: a new northern Red Sea deep. Origin and implications of continental rifting. Earth Planet Sci. Lett. 78, 18–32.
Cochran, J.R., 1983. A model for the development of the Red Sea. Bull. Am. Assoc. Pet. Geol. 67, 40–69.
David, S., Cronan, D., 1980. Underwater minerals. Academic Press. Technology & Engineering - 362 pages.
Girdler, R., Southern, T., 1987. Structure and evolution of the northern Red Sea. Nature 330, 716–721.
Izzeldin, A.Y., 1989. Transverse structures in the central part of the Red Sea and implications on early stages of Red Sea and implications in early stages of oceanic accretion. Tectonophysics 143, 269–306.
Krauskopf, K.B., 1957. Separation of manganese from iron in sedimentary processes. Geochim. Cosmochim. Acta 12 (1), 61–84.
Makris, J., Rihm, R., 1991. Shear-controlled evolution of the Red Sea: pull apart model. In: Makris, J., Mohr, P., Rihm, R. (Eds.), Red Sea: Birth and Early History of a new Oceanic Basin. Tectonophysics, vol. 198, pp. 441–446.
Pautot, G., Le Cann, C., Coutelle, A., Mart, Y., 1984. Decouverte d'une nouvelle fosse a saumures, sediments metalliferes et appareil vocanique central en Mer Rouge. Soc. Geol. Fr., 10e Reun. Ann. (Abstr.) 10, 435–436.
Pautot, G., Rangin, C., Briais, A., Tapponnier, P., Beuzart, P., Lericolais, G., Mathieu, X., Wu, J., Han, S., Li, H., Lu, Y., Zhao, J., 1986. Spreading direction in the central South China Sea. Nature (London, UK) 321 (6066), 150–154.
Roeser, H.A., 1975. A detailed magnetic survey of the southern Red Sea. Geol. Jahrb., Reihe D 13, 131–153.
Searle, R.C., Ross, D.A., 1975. A geophysical study of the Red Sea axial trough between 20·5° and 22°N. Geophys. J. Int. 43 (2), 555–572.
Shanks III, W.C., Bischoff, James L., Rosenbauer, Robert J., 1977. Seawater sulfate reduction and sulfur isotope fractionation in basaltic systems: Interaction of seawater with fayalite and magnetite at 200–350 °C. Geochim. Cosmochim. Acta 45 (11), 1977–1995.
Spieß, V., 1993. Digitale Sedimentechographie - Neue Wege zu einer hochauflösenden Akustostratigraphie. Berichte, Fachbereich Geowissenschaften, Universität Bremen 35, 1–199.
Wessel, P., Smith, W.H.F., 1999. The Generic Mapping Tools technical reference and cookbook. Version 3 (1), 90.
Winckler, G., Kipfer, R., Aeschbach-Hertig, W., Botz, R., Schmidt, M., Schuler, S., Bayer, R., 2000. Sub sea floor boiling of Red Sea Brines: new indication from noble gas data. Geochim. Cosmochim. Acta 64 (9), 1567–1575.